

# UNDERSTANDING SIGMA-DELTA MODULATION: The Solved and Unsolved Issues

By Joshua D. Reiss, AES Member

Sigma-delta modulation is the most popular form of analog-to-digital conversion used in audio applications. It is also commonly used in D/A converters, sample-rate converters, and digital power amplifiers. In this tutorial the theory behind the operation of sigma-delta modulation is introduced and explained. We explain how performance is assessed and resolve some discrepancies between theoretical and experimental results. We discuss the issues of usage, such as limit cycles, idle tones, harmonic distortion, noise modulation, dead zones, and stability. We characterize the current state of knowledge concerning these issues and look at what are the most significant problems that still need to be resolved. Finally, practical examples are given to illustrate the concepts presented.

## INTRODUCTION

Sigma-delta modulation (SDM) is perhaps best understood by comparison with traditional pulse-code modulation (PCM). A PCM converter typically samples an input signal at the Nyquist frequency and produces an  $N$ -bit representation of the original signal. This technique, however, requires quantization to  $2^N$  levels. Whether implemented using successive approximation registers, pipelined converters, or other techniques, high resolution is difficult to obtain in PCM conversion due to the need to accurately represent many quantization levels and the subsequent circuit complexity. This is the motivation for sigma-delta modulation, a form of pulse-density modulation, which exploits oversampling and sophisticated filter design in order to employ a low-bit quantizer with high effective resolution.

In this tutorial, we will consider common designs of sigma-delta modulators as used for analog-to-digital conversion. The basic principle is the same for SDMs employed in D/A or sample-rate conversion. We will restrict the analysis to asynchronous, discrete-time designs. However, these are by far the most common designs and include most feedforward, feedback, and multistage implementations. We will explain the theory of operation, emphasizing signal-to-noise ratio estimation and comparison with PCM conversion. We will also introduce the linear model, which assists in understanding filter design and noise shap-

ing principles. Since sigma-delta modulation is highly nonlinear, there are various phenomena that cannot be explained using this technique, such as instability and limit cycles. The literature on these phenomena can be confusing, so we attempt to give a clear definition of the terms and clarify the current state of understanding. Finally, we introduce several state-of-the-art techniques that can be used to deal with these unwanted phenomena.

## THE LINEAR MODEL AND PULSE-CODE MODULATION

The theory of quantization is well-established (see [1] and references therein). The allowed values in the

output signal, after quantization, are called quantization levels, whereas the distance between two successive levels, is called the quantization step size,  $q$ . For a quantizer with  $b$  bits covering the range from +1 to -1, there are  $2^b$  quantization levels, and the width of each quantization step is

$$q=2 / (2^b - 1) \quad (1)$$

This is depicted in Fig. 1 for a 3-bit quantizer.

The rounding, or midriser, quantizer assigns each input sample  $x(n)$  to the nearest quantization level. The quantization error is simply the difference between the input and output to the  $\blacktriangleleft$

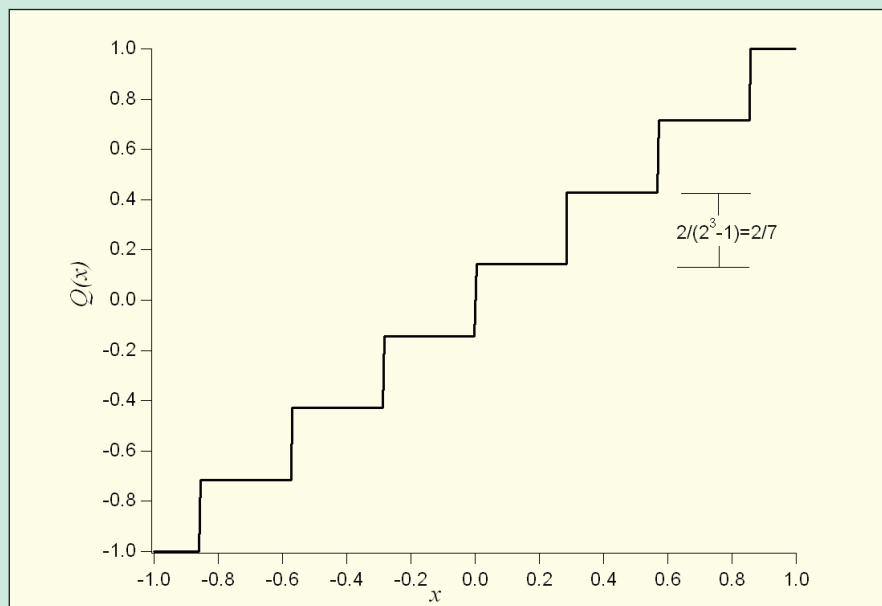


Fig. 1. Transfer characteristics for a 3-bit quantizer and V=1

quantizer,  $e_q = Q(x) - x$ . It can easily be seen that the quantization error  $e_q(n)$  is always bounded by

$$-q/2 \leq e_q(n) \leq q/2 \quad (2)$$

Since quantization is a highly nonlinear process, the exact effect of quantization on the signal content and the nature of quantization noise may be difficult to measure. For this reason, several assumptions are often made.

1. The error sequence,  $e_q(n)$ , is a stationary, random process.
2. The error sequence is uncorrelated with itself and with the input sequence  $x(n)$ .
3. The probability-density function of the error is uniform over the range of quantization error.

Such assumptions are known to be, in general, untrue. However, they are a reasonable approximation for large-amplitude, time-varying input signals when  $b$  is large and successive quantization error values are not highly correlated. Furthermore, as we shall see, results obtained through the use of this approximation yield accurate estimates of the signal-to-(quantization)-noise ratio, or SNR.

These assumptions allow us to represent quantization as the introduction of an additive white-noise source. This is depicted in Fig. 2. As we shall see, this model enables in-depth understanding of the signal and noise in quantization systems. More exact models exist that include gain terms applied to the signal and quantization noise, as in [2], but the model depicted here is sufficient for analysis.

The assumption that the quantization error is uniformly distributed over a quantization step gives

$$p(e_q) = \begin{cases} 1/q & |e_q| \leq q/2 \\ 0 & |e_q| > q/2 \end{cases} \quad (3)$$

Since the error is white noise, the power spectral density of the noise will also have a uniform distribution within the limits of the Nyquist band. The probability-density function and power spectral-density function are depicted in Figs. 3A and B respectively.

If the sampling rate satisfies the sampling theorem, i.e., the signal is sampled at least twice the highest frequency in the input signal,  $f_s > 2f_B$ , then quantization is the only error in the

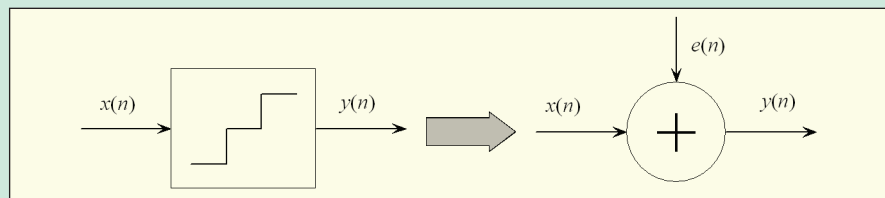


Fig. 2. The linear model of quantization

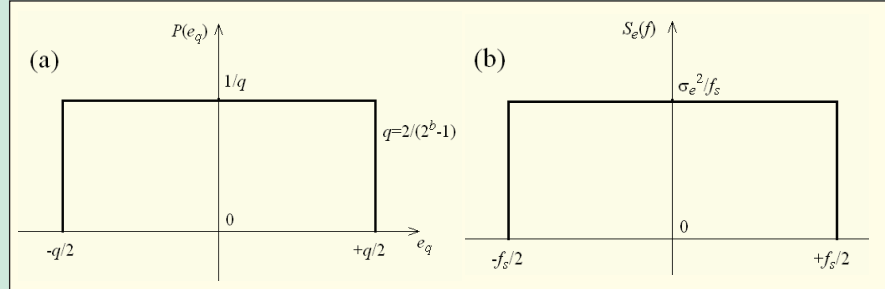


Fig. 3. (a) Probability-density function and (b) power spectral-density function for the quantization error under the linear model.

A/D conversion process (jitter and other effects are not considered here). Using the assumption of uniform distribution, the average quantization noise is given by

$$\bar{e}_q = E\{e_q\} = \int_{-\infty}^{\infty} e_q p(e_q) de_q = \frac{1}{q} \int_{-q/2}^{q/2} e_q de_q = 0 \quad (4)$$

and the quantization noise power is given by

$$\sigma_e^2 = E\{(e_q - \bar{e}_q)^2\} = \int_{-\infty}^{\infty} e_q^2 p(e_q) de_q = \frac{1}{q} \int_{-q/2}^{q/2} e_q^2 de_q = \frac{q^2}{12} \quad (5)$$

From (1), we get

$$\sigma_e^2 = \frac{q^2}{12} = \frac{1}{3(2^b - 1)^2} \approx \frac{1}{3 \cdot 2^{2b}} \quad (6)$$

To find the SNR, we also need to estimate the signal power. Now assume we are quantizing a sinusoidal signal of amplitude  $A$ ,  $x(t) = A \cos(2\pi t/T)$ . The average power of the signal is thus

$$\sigma_x^2 = E\{(e_x - \bar{e}_x)^2\} = E\{e_x^2\} = \frac{1}{T} \int_0^T (A \cos(2\pi t/T))^2 dt = \frac{A^2}{2} \quad (7)$$

From (6) and (7), the signal-to-noise ratio may now be given by,

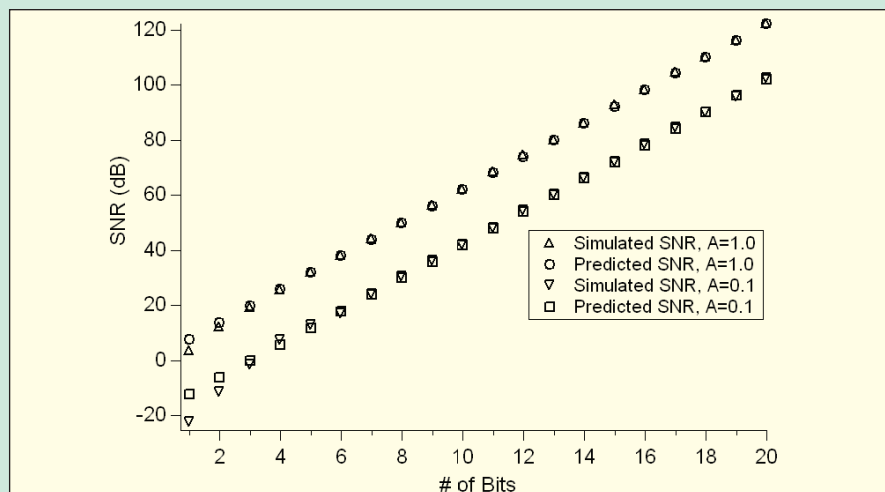


Fig. 4. SNR as a function of the number of bits in the quantizer for a PCM-encoded signal, sampled at the Nyquist frequency.



# AES is now a Scitopia.org partner

**one hundred fifty years of content**

**fifteen leaders in science & technology research**

**three million documents**

**one gateway to it all**

# scitopia.org

Search **scitopia.org** to find quality content from leaders in science and technology research. Scitopia.org generates relevant and focused results – with no Internet noise. From peer-reviewed journal articles and technical conference papers to patents and more, **scitopia.org** is a researchers' heaven on earth.

**search**

**scitopia.org**

Integrating Trusted Science + Technology Research

**Scitopia.org was founded by:** Acoustical Society of America • American Geophysical Union • American Institute of Physics • American Physical Society • American Society of Civil Engineers • American Society of Mechanical Engineers • American Vacuum Society • ECS • IEEE • Institute of Aeronautics and Astronautics • Institute of Physics Publishing • Optical Society of America • Society of Automotive Engineers • Society for Industrial and Applied Mathematics • SPIE

SNR(dB)=

$$20\log_{10} \frac{\sigma_x}{\sigma_e} \simeq 10\log_{10} \frac{3A^2 2^{2b}}{2} = \\ 20\log_{10} A + 6.02b + 1.76 \quad (8)$$

Thus the signal-to-noise ratio increases by approximately 6 dB for every bit in the quantizer. Using this formula, an audio signal encoded onto CD (a 16-bit format) using PCM, has a maximum SNR of 98.08. Also note from (7) that the SNR is linearly related to the signal strength in decibels.

In Fig. 4, the SNR is given as a function of the number of bits in the quantizer for two PCM encoded signals, sampled at the Nyquist frequency. Eq. (8) is used to predict the SNR, and the simulated SNR is measured directly in the time domain from signal variance and quantization-error variance. The input signals are 2-kHz sinusoids, where it is assumed that the sampling rate is 44.1 kHz, with full range amplitude  $A=1$  and with small amplitude  $A=0.1$ . It can easily be seen, for a high-bit quantizer, that the signal-to-noise ratio is indeed given by Eq. (8). The only significant error is for a low number of bits due to the approximation first introduced in Eq. (6).

Eq. (8) also gives a method by which the performance of sigma-delta modulators may be compared with Nyquist-rate PCM converters. By inverting this formula for a full-scale input signal and incorporating all the noise and distortion into the signal-to-noise-and-distortion ratio (SINAD), we have the measurable effective number of bits of a quantization,

$$ENOB = \frac{SINAD-1.76}{6.02} \quad (9)$$

## NOISE SHAPING AND OVERSAMPLING

Let's now assume that the signal is oversampled. That is, rather than acquiring the signal at the Nyquist rate,  $2f_B$ , the actual sampling rate is  $f_s=2^{r+1}f_B$ . The oversampling ratio is  $OSR=2^r=f_s/2f_B$ . Thus, the quantization noise is spread over a larger frequency range yet we are still primarily concerned with noise below the Nyquist frequency.

The in-band quantization noise power

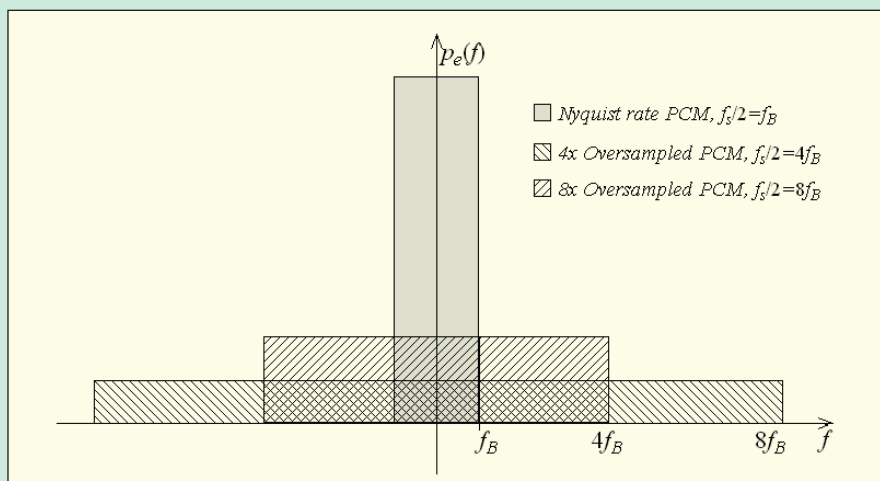


Fig. 5. Distribution of quantization noise for Nyquist rate sampling, 4 times, and 8 times oversampling

can be found by integrating the power spectral density over the passband,

$$\sigma_n^2 = \int_{-f_B}^{f_B} S_e(f) df = \\ \frac{2\sigma_e^2 f_B}{f_s} = \sigma_e^2 / OSR \quad (10)$$

where  $S_e(f) = \sigma_e^2 / f_s$  is the power spectral density of the (unshaped) quantization noise.

Most of the noise power is now located outside of the signal band. As depicted in Fig. 5, the quantization-noise power within the band of interest has decreased by a factor  $OSR$ . The signal power occurs over the signal band only, so it remains unchanged and is given by Eq. (7). The signal-to-noise ratio may now be given by,

$$SNR(dB)= \\ 10\log_{10} \frac{\sigma_x^2}{\sigma_e^2} + 10\log_{10} 2^r \simeq \\ 20\log_{10} A + \\ 6.02b + 3.01r + 1.76 \quad (11)$$

Thus for every doubling of the oversampling ratio, the SNR improves by 3 dB. The 6-dB improvement with each bit in the quantizer remains, so we can say that doubling the oversampling ratio increases the effective number of bits by half a bit.

Oversampling gives us a means to reduce the required number of bits in the quan-

tizer. However, this alone is not sufficient. According to Eq. (11), to achieve a CD-quality recording (ENOB=16,  $f_s=44,100$  kHz) with an 8-bit quantizer we would need an oversampling ratio of 216, or sample rate of approximately 2.89 GHz, which is unfeasible.

## STF and NTF under the linear model

The above oversampling system performs no noise shaping. Consider a filter placed in front of the quantizer (known as the loop filter), and the output of quantization is fed back and subtracted from the input signal, as shown in Fig. 6. We now have a system that may be represented by transfer functions applied to both the input signal and the quantization noise. In the Z domain, the output may be represented as

$$Y(z) = \\ STF(z)X(z) + NTF(z)E(z) \quad (12)$$

where STF is the signal transfer function and NTF is the noise transfer function. To find these values, note that the input to the loop filter is  $X(z)-E(z)$  so that  $Y(z)=H(z)[X(z)-Y(z)]+E(z)$ .

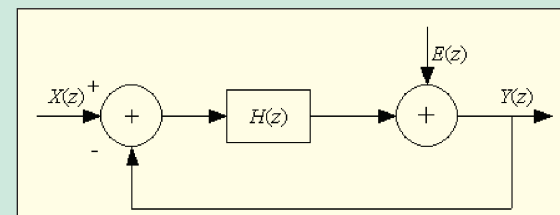


Fig. 6. Representation of a sigma-delta modulator using the linear model

Rearranging terms, we have,

$$Y(z)[1 + H(z)] = H(z)X(z) + E(z) \quad (13)$$

And thus,

$$\begin{aligned} STF(z) &= \frac{H(z)}{1 + H(z)}, \\ NTF(z) &= \frac{1}{1 + H(z)} \end{aligned} \quad (14)$$

So the linear model allows us to find the effects on the signal and noise due to any choice of filter function.

This filtering and feedback, combined with oversampling, are the essential elements of sigma-delta modulation. The primary goal of sigma-delta modulator design is to choose a filter resulting in high stability and few artifacts, such that over the passband,

$$STF(z) \approx 1, \quad NTF(z) \approx 0 \quad (15)$$

If such is the case, then the noise has been shaped away from the passband and the signal passes unchanged.

### First-order sigma-delta modulation A/D converter

A first-order SDM has a single integrator in the loop filter. The simplest design has no additional gain terms and may be given in the time domain as,

$$u(n+1) = x(n) - y(n) + u(n) \quad (16)$$

which is depicted in the block diagram Fig. 7A). Recalling that,  $e_q = Q - u$  and describing the previous time step, we have

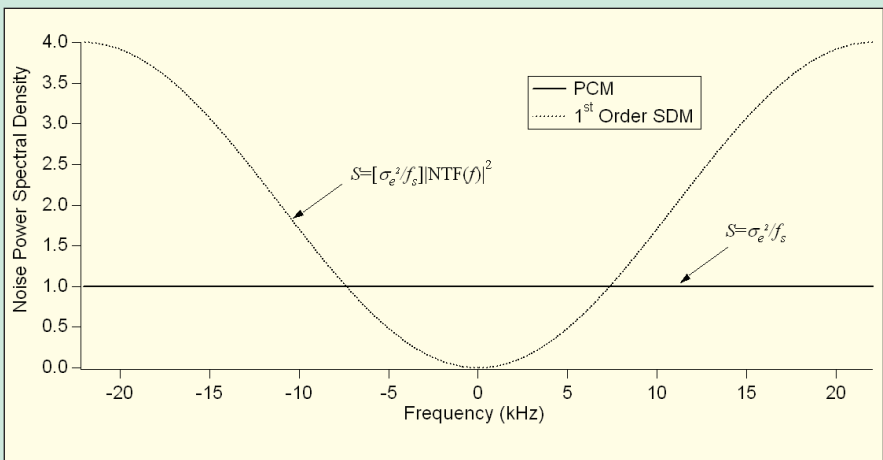


Fig. 8. Normalized power spectral density for pulse-code modulation and for first-order SDM (no oversampling). Actual values are found by multiplying by  $\sigma_e^2 / f_s$ .

$$y(n) = x(n-1) + e_q(n) - e_q(n-1) \quad (17)$$

A Z-domain block diagram is given by Fig. 7B, and the corresponding equation is

$$Y(z) = X(z)z^{-1} + E(z)(1 - z^{-1}) \quad (18)$$

Thus the signal transfer function is given by  $z^{-1}$ . The signal is unaffected and only delayed by one sample. The noise transfer function is  $1 - z^{-1}$ , which pushes the noise to high frequencies. Using trigonometric identities,

$$\begin{aligned} |NTF(f)|^2 &= \\ (1 - e^{-j2\pi f/f_s})(1 - e^{j2\pi f/f_s}) &= \\ 4\sin^2(\pi f/f_s) \end{aligned} \quad (19)$$

Unlike oversampled PCM, which has unity NTF, the noise shaping in sigma-delta modulation implies a nonconstant noise power, given in the

baseband by,

$$\sigma_n^2 = \int_{-f_B}^{f_B} S_e(f) |NTF(f)|^2 df \quad (20)$$

where, again,  $S_e(f) = \sigma_e^2 / f_s$  is the power spectral density of the unshaped quantization noise. The total noise power,  $\sigma_n^2$ , remains unchanged, but now the noise has been pushed up to the high frequencies. This is depicted in Fig. 8, which gives the power spectral density for first-order SDM as compared with PCM.

Assuming a high OSR,  $f_s \gg f_B$  and using a Taylor series expansion,  $\sin(x) = x - x^3/3! + x^5/5! \dots$ , Eq. (20) can be solved to give

$$\begin{aligned} \sigma_n^2 &= \\ \frac{\sigma_e^2}{f_s} \left[ 4f_B - \frac{2f_s}{\pi} \sin(2\pi f_B / f_s) \right] &\approx \\ \frac{\pi^2}{3 \cdot OSR^3} \sigma_e^2 \end{aligned} \quad (21)$$

The signal-to-noise ratio may now be given by,

$$\text{SNR(dB)} = 10 \log_{10} \frac{\sigma_x^2 3 \cdot 2^{3r}}{\sigma_e^2 \pi^2} \approx 20 \log_{10} A + 6.02b + 9.03r - 3.41 \quad (22)$$

The effect of first-order noise shaping is evident. We now get an improvement of 9 dB for each doubling of the oversampling ratio, rather than the 3-dB improvement that occurs without noise shaping.

### SNR for high-order sigma-delta modulators

This technique can be extended to higher-order filters. The transfer

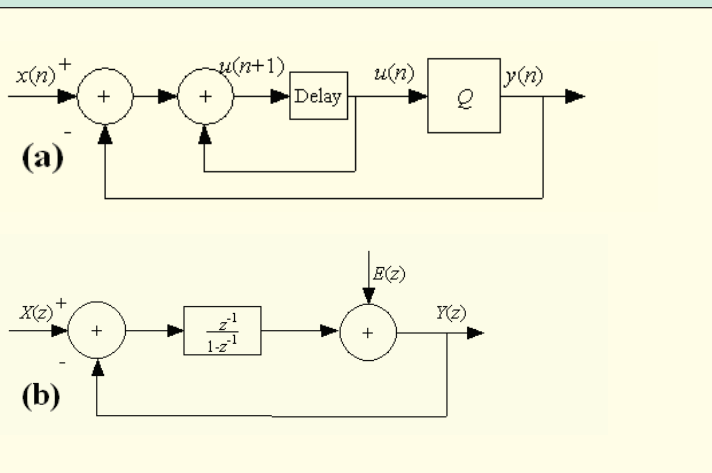


Fig. 7. (a) first-order sigma-delta modulator given by its block diagram and alternatively (b), by its z-transform block diagram with the quantizer approximated by a noise source.

function of a generic Nth-order SDM is given by

$$Y(z) = X(z)z^{-1} + E(z)(1-z^{-1})^N = STF(z)X(z) + NTF(z)E(z) \quad (23)$$

Thus, the noise transfer function is given by

$$NTF(f) = (1 - e^{-j2\pi f/f_s})^N \quad (24)$$

Using an integral formula, this gives

$$\begin{aligned} \sigma_n^2 &= \int_{-f_B}^{f_B} S_e(f) |NTF(f)|^2 df = \\ &\frac{\sigma_e^2}{f_s} \int_{-f_B}^{f_B} [2 \sin(\pi f / f_s)]^{2N} df \approx \\ &\sigma_e^2 \frac{\pi^{2N}}{(2N+1)OSR^{2N+1}} \end{aligned} \quad (25)$$

where the approximate equality was found by using a Taylor series expansion on the sine terms and keeping only the first nonzero terms.

Compared with the first-order SDM, this provides more suppression of the quantization noise over the low frequencies and more amplification of the noise outside the signal band. Eq. (25) can be used to find the general formula for the SNR of an ideal Nth-order SDM,

$$\begin{aligned} \text{SNR(dB)} &= 10 \log_{10} \frac{\sigma_x^2}{\sigma_e^2} + \\ &10 \log_{10} \frac{(2N+1)2^{(2N+1)r}}{\pi^{2N}} \approx \\ &20 \log_{10} A + 6.02b + 1.76 + \\ &10 \log_{10}(2N+1) - 9.94N + \\ &3.01(2N+1)r \end{aligned} \quad (26)$$

Thus we see a large improvement with increasing SDM order. For a second-order SDM ( $N=2$ ), there is a 15-dB improvement in the SNR with each doubling of the oversampling ratio, and a 6-dB improvement with each additional bit in the quantizer. Thus, use of high-order SDMs and a high oversampling ratio offers a much better SNR than that obtained by simply increasing the number of bits.

In general, for an  $N$ th-order SDM, there is a  $3(2N+1)$  dB improvement in the SNR with each doubling of the oversampling ratio, and a 6-dB improvement with each additional bit in the quantizer. Thus, use of high-order SDMs and a high oversampling ratio offers a much better SNR than that obtained by simply increasing the number of bits.

Of course, this is an approximation. It depends on the coefficients of the modulator, on the approximations used in the derivation, and other factors. Nevertheless, it provides an

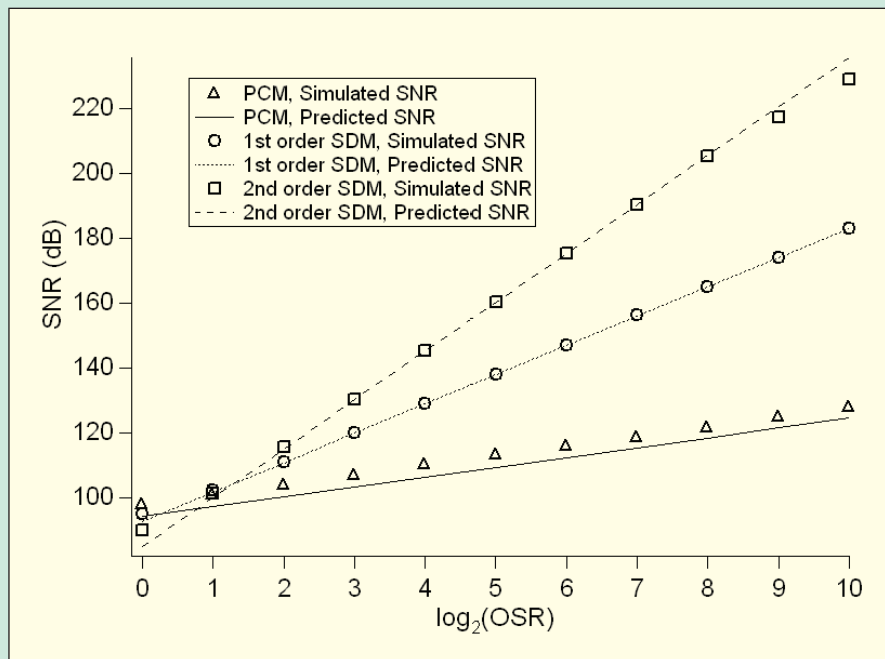


Fig. 9. SNR as a function of  $r$ , the  $\log_2$  of the oversampling ratio. In each case,  $2^{17}$  samples and a 16-bit quantizer were used, and the input signal had a frequency  $101f_s/2^{17}$ .

upper limit on the SNR. Fig. 9 depicts the SNR for PCM encoding, a first-order SDM, and a second-order SDM. In each case  $2^{17}$  samples and a 16-bit quantizer were used, and the input signal had a frequency  $101f_s/2^{17}$ . Unlike in the PCM simulation for Fig. 4, the quantization error and input signal samples are no longer time aligned, so the signal and noise power were calculated in the frequency domain. There is strong agreement between theory and simulation, with the differences being attributable to the assumption of high oversampling ratio (for the Taylor series truncation), the difficulty in accurate measurement of SNR, particularly at large values, and the assumptions mentioned

earlier, particularly that of uniform PDF over the range  $-q/2$  to  $+q/2$ . Nevertheless, the 3-dB, 9-dB, and 15-dB increases for doubling the OSR have been confirmed, and there is reasonable agreement throughout.

## ISSUES IN SIGMA-DELTA MODULATION

As reported in [3, 4], 64-times-over-sampled 1-bit A/D converters, using a fifth-order SDM have been designed and achieve an SNR over 120 dBs. Yet from Eq. (26), we find that

$$\text{SNR(dB)} \approx 20 \log_{10} A + 167.15 \quad (27)$$

To date, no one has designed a sigma-delta modulator with such high performance. As an example, consider

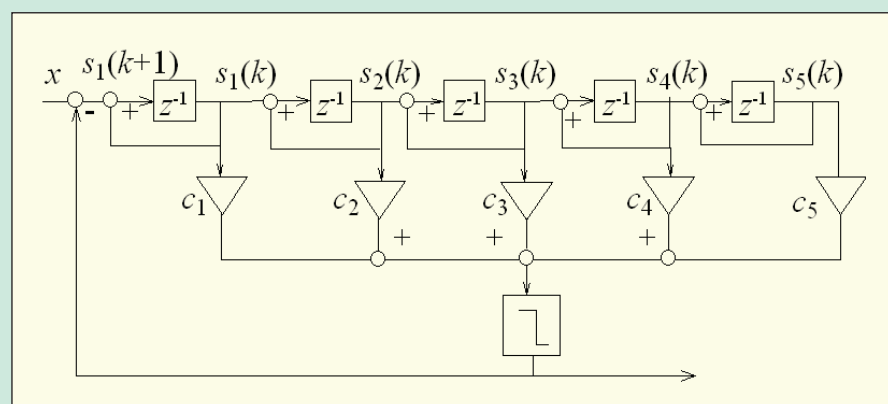


Fig. 10. Implementation of a realistic fifth-order feedforward SDM

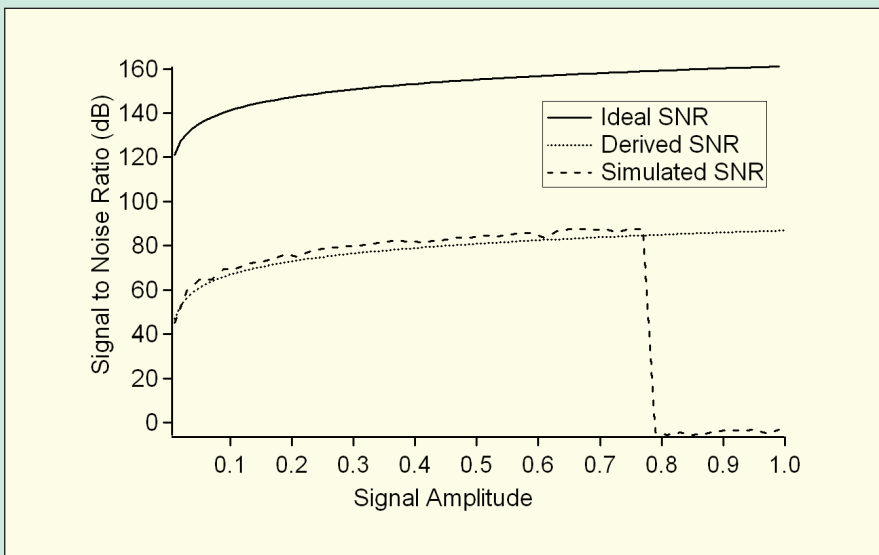


Fig. 11. Estimates of the signal-to-noise ratio as a function of input signal amplitude for an ideal SDM, derived from theory, and for a practical SDM, both derived from theory and estimated from simulation. In all cases, the SDM was assumed to be 1-bit, fifth-order, with an oversampling ratio of 64.

a 1-bit, arbitrary-order feedforward SDM that may be represented as,

$$\begin{aligned} y(n) &= \text{sgn}(\mathbf{c} \cdot \mathbf{s}(n)) \\ s_1(n+1) &= s_1(n) + x(n) - y(n) \\ s_2(n+1) &= s_1(n) + s_2(n) \\ \dots \\ s_N(n+1) &= s_{N-1}(n) + s_N(n) \end{aligned} \quad (28)$$

$x$  is the input signal and  $y$  the output bitstream, as before, and  $u = \mathbf{c} \cdot \mathbf{s}$  is the input to the quantizer, where  $\mathbf{c}$  is a coefficient vector determining noise-shaping characteristics. A practical fifth-order implementation of this design, Fig. 10, is described in [5], and is intended to be used for analog-to-digital conversion in audio applications (we will return to this SDM later in this section to demonstrate other phenomena). The SDM is lowpass, has a corner frequency of 80 kHz for a sample rate of  $64 \times 44.1$  kHz, and is given by the coefficients,

$$\begin{aligned} \mathbf{c} = &[0.5761069262, \\ &0.1624753515, \\ &0.0276093301, \\ &0.0028053934, \\ &0.0001360361] \end{aligned} \quad (29)$$

Fig. 11 depicts the theoretical SNR as a function of input signal amplitude for an ideal fifth-order SDM, and both theoretical and simulated SNR estimates for the SDM given by Eq. (28) and (29). In both cases, the SDM was assumed to be 1 bit with an oversam-

pling ratio of 64. The theoretical SNR is computed directly from the signal power and in-band noise power. In-band noise power is found from the integral given by Eq. (20), which is numerically integrated for the practical SDM and may be found from Eq. (26) for the ideal SDM. Note that the practical design has an SNR almost 80 dB less than that of the ideal design, and that simulation shows a dramatic drop in performance for input amplitude greater than 0.77.

The archetypal  $N$ th-order SDM with  $NTF(1-z^{-1})^N$  is highly unstable; hence loop filters with less-aggressive noise shaping are used. But even this less-aggressive SDM becomes unstable with large input values. This instability problem is not explained by the linear model. In fact, there are a host of issues in sigma-delta modulation that are caused by feedback around a highly nonlinear quantizer. In this section we will look at the related causes of these unwanted behaviors and highlight the current state of understanding and research.

### Limit cycles

Consider a single-bit

first-order SDM as given by Eq. (16) with constant input  $x=.5$ , and an initial condition, say,  $u(n)=0.1>0$

$$\begin{aligned} u(n+1) &= .5 - 1 + .1 = -.4 \\ u(n+2) &= .5 + 1 - .4 = 1.1 \\ u(n+3) &= .5 - 1 + 1.1 = .6 \\ u(n+4) &= .5 - 1 + .6 = .1 \end{aligned} \quad (30)$$

Thus, the input to the quantizer repeats with a period of 4 iterations and the quantizer produces a repeating output bitstream  $+1,-1,+1,+1\dots$ . Note that the average value is  $[3*(+1)+1*(-1)]/4$ , which is the same as the input. This relationship can be easily shown for a first-order SDM since repeated application of Eq. (16), leads to

$$u(n+k) = \sum_{i=0}^{k-1} x(n+i) - \sum_{i=0}^{k-1} y(n+i) + u(n) \quad (31)$$

If we assume constant input and that  $u$  repeats after  $k$  cycles, we have

$$kx = \sum_{i=0}^{k-1} y(n+i) \quad (32)$$

which implies that average output is equal to the input signal. The occurrence of a repeating sequence in the output bitstream is known as a limit cycle. It poses problems in the signal processing of the output. More seriously, when SDMs are applied in audio applications, limit cycles can result in audible artifacts. For instance, in the case just mentioned, the input was purely DC, yet the limit cycle results in a square wave with 75% duty cycle and frequency  $f_s/4$  at the output.

The theory of limit cycles in low-

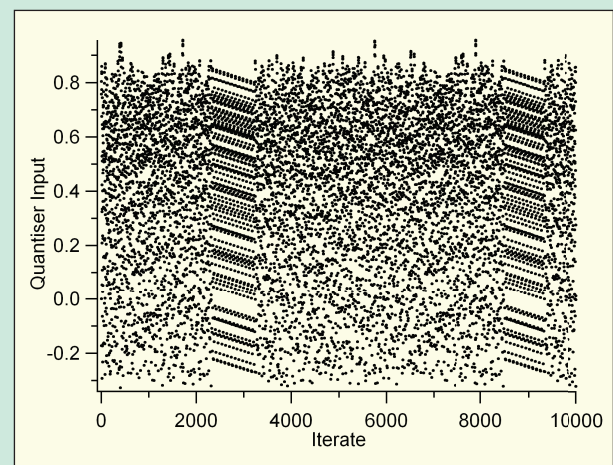


Fig. 12. Plot of the input to the quantizer as a function of the iterate for a fifth-order SDM. The quantizer input, and hence the output bitstream, enter a limit cycle around iterate 2300 and again at approximately 8400.

order (first- and second-order) sigma-delta modulators is well understood. Yet limit cycles can exist in high-order SDMs operating under normal conditions. Returning to the SDM described in the introduction at the beginning of this section, with an input of 0.7 and initial conditions  $s=0$ , it exhibits a short-term limit cycle. This can be seen in a time series of the input to the quantizer, as depicted in Fig. 12. This example illustrates both the existence of limit cycles in high-order designs and the fact that limit cycles may also appear for finite duration.

It is only in recent years that the theory of limit cycles has been extended to characterize behavior in higher-order SDMs [5–10]. Reefman's Theorem shows that, for most SDM designs, DC input implies that the output bitstream is periodic if and only if the state-space variables (a vector describing the current state of the system) are periodic. Using this condition it was possible to find all limit cycles that may occur for a given sigma-delta modulator and the set of initial conditions that may generate them. This allowed a description of sensitivity to limit cycles for different SDM designs and the ease by which various techniques may be used to break out of a limit cycle. Other significant recent results include analysis of limit-cycle behavior with nonconstant, periodic input and development of limit-cycle detection and removal techniques.

Design of SDMs to avoid limit cycles is accomplished either by using more complex noise shaping structures [11] or through the addition of dither or a control [12] in order to suppress limit cycles in an existing design. Questions linger concerning how problematic limit cycles are when the input has a small amount of noise, such as with analog implementations of SDMs when the limit cycle is of finite duration or when the input is not constant but the oversampling ratio is large enough such that the input appears nearly constant over a short duration. The framework established in [5] may be used to address these issues.

### Idle tones

There is little theoretical understanding of idle tones, even for the simplest

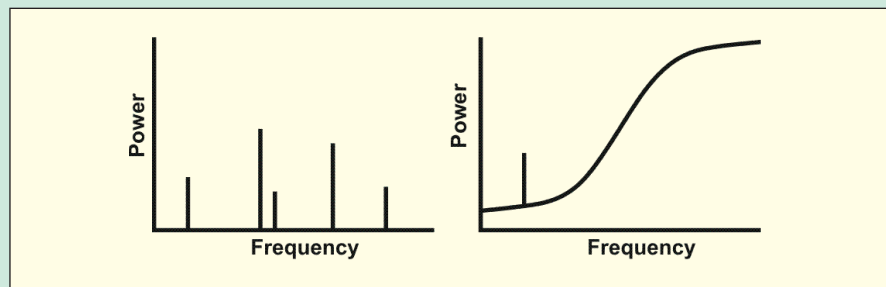


Fig. 13. Illustration of the definitions used to distinguish a limit cycle (left) from an idle tone (right). A limit cycle consists of a finite number of discrete peaks in the frequency spectrum; an idle tone is a peak in the frequency spectrum, but superimposed on a noise background.

low-order sigma-delta modulators. Perhaps the most significant is early work by Candy [13] that showed that in a first-order SDM the idle tone is simply an alias of an overtone of a square wave that is discretely sampled. Thus it is suspected that a similar phenomenon may account for idle tones in higher-order SDMs. The idle-tone phenomenon in higher-order SDMs has been described in [14, 15], and experimental evidence of idle-tone behavior in a second-order bandpass SDM was reported in [16].

It is important to distinguish between limit cycles and the related phenomenon of idle tones. The repetitive patterns that exist in the output bitstream are referred to as idle patterns or limit cycles. Whereas an idle tone is represented by a discrete peak in the frequency spectrum of the output of a SDM, but superimposed on a background of noise (see Fig. 13). In

this case there is no unique series of repeating bits.

This distinction is often blurred, and alternative definitions are sometimes used. Kozak and Kale [17] do not distinguish between limit cycles and idle tones per se, but instead refer to idle tones as periodic patterns with constant input and harmonic tones as periodic patterns resulting from sinusoidal input.

Bourdopoulos [18] reported idle tones occurring with both constant and sinusoidal input for a third-order SDM. The latter we would refer to as harmonic distortion. He also linked the generation of idle tones to the existence of almost repeating patterns. Ledzius [19] used this link to infer that since a linear model of an SDM cannot account for limit cycles, it must not be able to account for idle tones either. This link to limit cycles (exactly periodic sequences) has also been suggested by Angus [20] and ↗

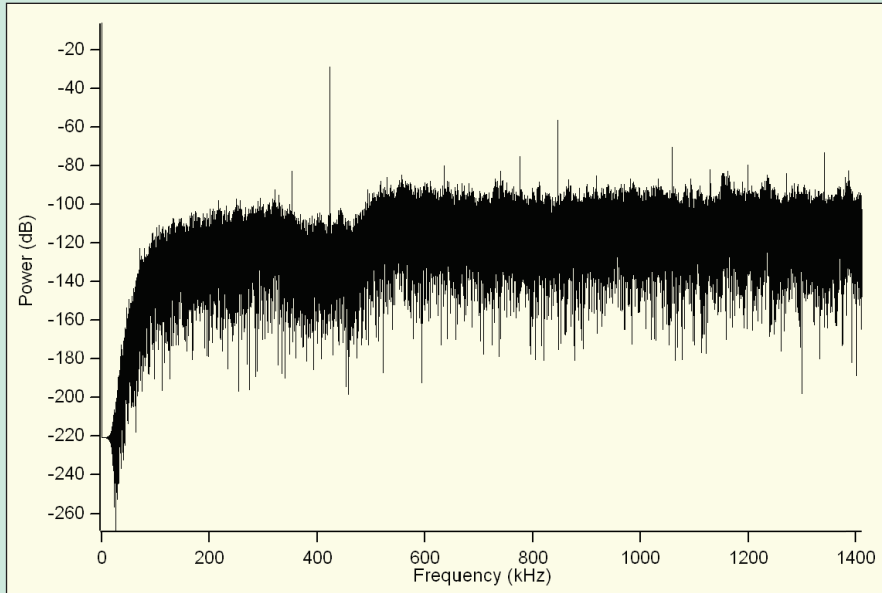


Fig. 14. Power spectrum of a 64 times oversampled fifth-order SDM with constant input of amplitude 0.7, depicting idle tones.

# ASSISTANT PROFESSOR of AUDIO ENGINEERING TECHNOLOGY

- ❑ Teach 24 credit hours per year.
- ❑ Advise students with academic progress and mentor students in research and other class-related activities.
- ❑ Engage in activities to support the mission and vision of Belmont University and the College.
- ❑ Engage in scholarly activity and professional development.
- ❑ Participate in departmental work as appropriate.

For additional information about the position and to complete the online application, visit <http://jobs.belmont.edu>.

Review of applications will begin immediately. Belmont University is an equal opportunity /affirmative action employer under all applicable civil rights laws.

Women and minorities are encouraged to apply.

Located near Nashville's Music Row, the Mike Curb College of Entertainment and Music Business at Belmont University enrolls 1200+ majors and combines classroom experience with real-world applications. Facilities feature state-of-the-art classrooms and recording studios, including the award-winning Ocean Way Nashville studios, Historic RCA Studio B, and the Robert E. Mulloy Student Studios in the Center for Music Business.



MIKE CURB COLLEGE of  
ENTERTAINMENT & MUSIC BUSINESS  
**BELMONT**  
UNIVERSITY

Jespers [21]. Yet recent work by the authors has shown that, although these tones are related to the input in much the same way as for limit cycles, they are not easily accounted for within the current theory of limit cycles [9].

However tempting, the assumption that idle tones result from limit cycles has so far left several phenomena unexplained. First, the limit cycle produces a spectrum with discrete peaks of comparable amplitude occurring at multiples of the limit-cycle frequency [9]. Thus, for a limit cycle with a short period, all peaks would be out of the audible band. For a limit cycle with sufficiently long period to produce audible tones, almost all harmonics would be present and significant. This is in direct contrast to idle tones, which are known to produce a relatively small number of peaks and the higher harmonics are of small amplitude. Furthermore, limit cycles are highly sensitive to initial conditions and input. An infinitesimal change in the input will completely remove a limit cycle, and a change in initial conditions will destabilize it. Idle tones, on the other hand, may be observed regardless of initial conditions and persist as the input is changed. Finally, it has been shown that limit cycles exist only if the input is constant or periodic [6] whereas there are no known similar constraints on idle tones.

The phenomenon of idle tones is illustrated in Fig. 14, which depicts the power spectrum of the fifth-order SDM described in the previous section on limit cycles, with constant input of 0.7. The strongest idle tone occurs at 423.36 kHz, or exactly 3/20 of the sampling frequency of 64 x 44.1 kHz. The next strongest is the first harmonic of this tone. This is also evidence of a simple relationship observed in [22]. In that paper the authors noted that the frequency of the fundamental idle tone, referred to as  $f_{FIT}$ , is proportionally related to the amplitude of the input signal,

$$f_{FIT} = A_{DC} f_s \quad (33)$$

Here, we refer to the amplitude as related to full scale. An input of amplitude 0.7 is 17/20 of the full scale from -1 and +1, or 3/20 of the full scale on a reverse x-axis, from +1 to -1. Since  $17f/20$  is above  $f_s/2$ , we would expect

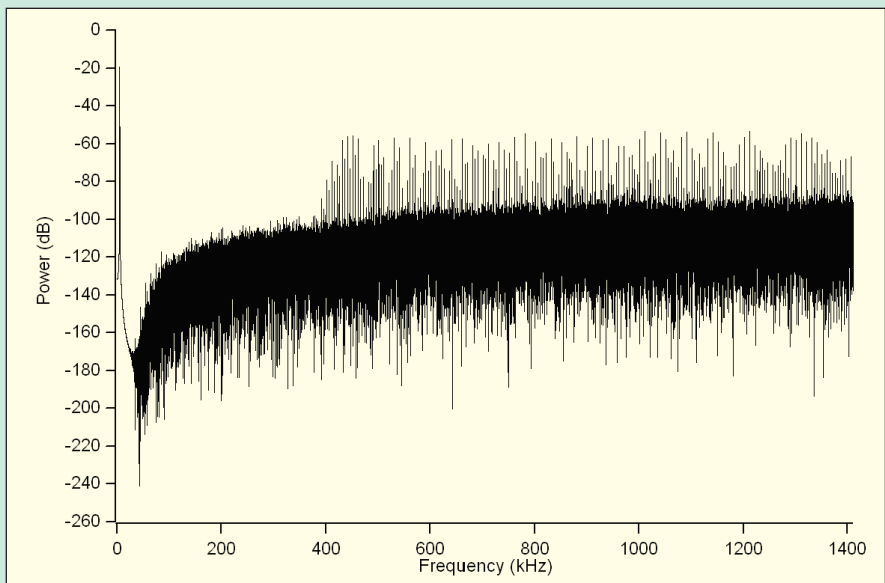


Fig. 15. Power spectrum of a 64 times oversampled fifth-order SDM with sinusoidal input of frequency 5 kHz and amplitude 0.7, depicting harmonic distortion.

the frequency of the idle tone to be  $3f_s/20$ , as observed. The other significant idle tones are due to harmonics and aliasing of the fundamental tone. Although the fundamental idle tone is typically far outside the audible range, higher-order harmonics of this tone may alias back to lower frequencies.

It is important to note that the relationship given by Eq. (33), though easily observed, has no known theoretical justification. Nor does there yet exist any theory that will estimate the amplitudes of the idle tones. This is perhaps more relevant since the designer is concerned with unwanted tones that are significantly above the noise floor. Furthermore, the fundamental and its harmonics may not account for all observed tones. Thus a more detailed understanding of idle tones remains a significant challenge.

Proposed solutions to idle tones and harmonic distortion are the addition of dither or the use of chaotic SDMs [23]. These same solutions are effective in eliminating limit-cycle behavior. Thus, it is believed that these are, at least in part, dynamical systems phenomena, but not a direct consequence of limit cycles. Nonlinear dynamics techniques may therefore be successful in devising a parallel analytical approach to the understanding of idle tones.

### Harmonic distortion

As with idle tones, there are multiple definitions of harmonic distortion in

the literature. Harmonic distortion, though also appearing as undesired tones, occurs when sinusoidal input is applied. It may be defined as the presence of harmonics (signals whose frequencies are integer multiples of the input signal) and other spurs in the output spectrum that were not present in the input signal. In this case we are concerned both with peaks that are due to unwanted harmonics or aliasing of the input signal and those that bear no apparent relationship to the input frequency.

Kozak and Kale [17] refer to harmonic tones as periodic patterns resulting from sinusoidal input (these would still be considered limit cycles under our previous definition). Experimental evidence of harmonic distortion was given in [24] and [25]. Theoretical results have typically been limited to approximate analysis of second-order or third-order harmonics [26] or low-order modulators [13, 27]. They are also specific to harmonic distortion that appears as a result of circuit imperfections, as opposed to the inherent distortion components in high-order SDMs. Aliasing of the distortion components back into the passband was described in [28], though no theoretical approach was provided.

Harmonic distortion is depicted in the power spectrum shown in Fig. 15, which is identical to Fig. 14 except now the constant input of 0.7 has been replaced with sinusoidal input of

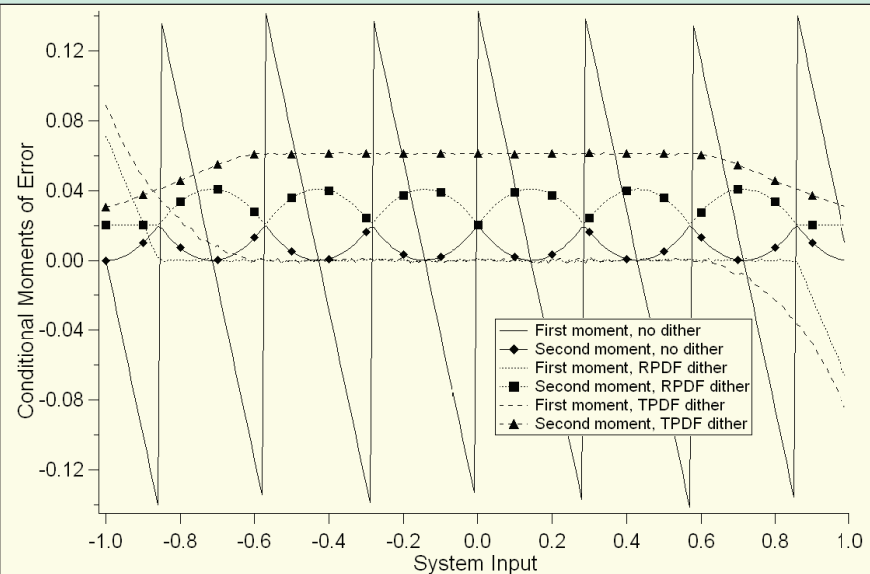


Figure 16. The first two conditional moments of error (average quantization noise and average quantization noise power)

amplitude 0.7. The distortions are far more numerous than the idle tones produced from constant input and are especially intriguing because they show no obvious relationship to the input frequency or amplitude. In both cases, fortunately, the tones are far outside the audio band (though this is not always the case).

Harmonic distortion, even though it is a serious issue, is not well understood. It is known that it is more problematic in low-order designs, and the same techniques that are used to remove idle tones may be applied here. The origins of harmonic distortion lie in the fact that, in a low-bit representation, sinusoidal signals are represented in the output bitstream as close to a square wave. Since square waves have strong harmonics, these harmonics appear in the output spectrum. However, no general theory exists allowing one to analytically derive the dominant harmonics and their amplitudes or to determine the susceptibility of different filter designs to harmonic distortion.

### Noise modulation

We begin by looking at dither distributions and the resultant quantization error in PCM systems. The approach used is slightly simpler though less rigorous than that in [1]. The analysis in this section is presented primarily because the analysis of SDM systems can be made via an extension of this approach.

Recall that an infinite midriser

quantizer has the input-output characteristic  $Q(w) = q \lfloor w/q \rfloor + q/2$ , where  $w$  is the input to the quantizer. If the input to a PCM system,  $x$ , is fed directly into the quantizer, then the total error between input and output is simply

$$e_q = q \lfloor x/q \rfloor + q/2 - x \quad (34)$$

Thus the  $m$ th moment of the error for a given  $x$  is

$$\sum e_q p(e_q) = (q \lfloor x/q \rfloor + q/2 - x)^m \quad (35)$$

Under such circumstances, all error moments are dependent on the input value  $x$ . In particular, the second moment, the quantization noise power, depends on the signal. This is known as noise modulation. It can be perceived in the quantization of audio signals and is generally undesirable.

However, if random noise with uniform probability distribution from  $-q/2$  to  $+q/2$ , otherwise known as rectangular PDF (RPDF) dither of size 1 Least Significant Bit (LSB), is applied immediately before quantization then the PDF of the input to the quantizer has the form,

$$p(w) = \begin{cases} 1/q & x - q/2 < w \leq x + q/2 \\ 0 & \text{otherwise} \end{cases} \quad (36)$$

The input ranges over 1 LSB, so the output can assume only 2 possible values. If we define  $y = x/q + 1/2 - \lfloor x/q + 1/2 \rfloor$ , then the error has the distribution,

$$e_q = \begin{cases} q(1-y) & p = y \\ -qy & p = 1-y \end{cases} \quad (37)$$

and hence, using Eq. (35), the first error moment becomes independent of the input.

$$\sum e_q p(e_q) = q(1-y)y - qy(1-y) = 0 \quad (38)$$

Note that this was also the result of the uniform distribution assumption in the linear model, Eq. (4), only now the addition of dither makes the assumption fully valid. In fact, it can be shown that  $n$ th-order dither will make the first  $n$  error moments independent of the input. Triangular (TPDF) dither of width 2 LSBs, which can be generated by summing two rectangular PDF dithers of width 1 LSB, will render both the first- and second-order moments of the error independent of the input signal. That is, the quantization noise will have a constant average of zero and a constant (nonzero) power independent of the input signal characteristics. The dithering forces the quantization noise to lose its coherence with the original input signal, but has the drawback of raising the average spectral noise floor.

The effect of dither on the conditional moments of error is depicted in Fig. 16. This shows the first two conditional moments of error (average quantization noise and average quantization noise power) as a function of the system input for a PCM system without dither, with RPDF dither and with TPDF dither. This PCM system uses the same 3-bit midriser quantizer as depicted in Fig. 1. The results were found from simulation of 100,000 data points with a constant input to the system and a random number generator used to create the dither signal. With RPDF dither, the average quantization noise remains fixed at zero, regardless of the input signal. With TPDF dither both the average quantization noise and the average quantization noise power are constant, thus the noise modulation has been removed. However, due to the finite bits in the quantizer, the results do not hold for the lowest and highest quantization levels with RPDF dither, and do not hold for the lowest two and highest two quantization levels with TPDF dither.

To date, the theory of noise ➤

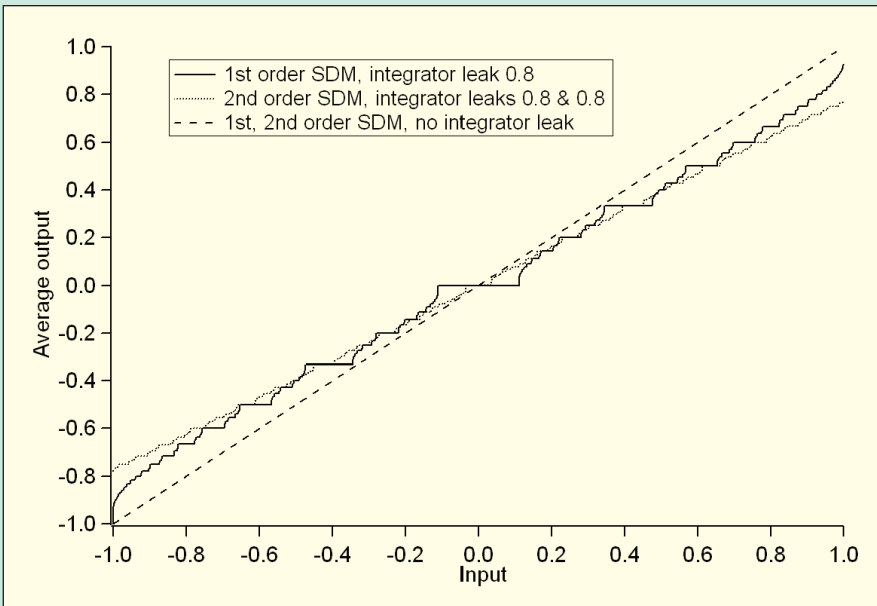


Fig. 17. Average output as a function of DC input for first- and second-order SDMs with integrator leak

modulation has not yet been extended from PCM to SDM. Though the use of dither to prevent noise modulation in pulse-code modulation is well understood, there are many intriguing questions that remain when dither is applied to a sigma-delta modulation system. The feedback loop affects the distribution of the input to the quantizer in complicated ways. Many researchers have suggested that this leads to a form of “self-dithering,” but correlations remain between the quantization noise and the input signal. In addition, one-bit sigma-delta modulation is frequently used, yet RPDF dither of 1 LSB or TPDF dither of 2 LSBs, as mentioned above, will cause the quantizer to be overloaded [29], and no amount of dither in a one bit system will produce constant noise power [30].

### Dead zones

For certain input signals, the input may not be properly encoded by the SDM. That is, there is a range of input for which the sigma-delta modulator may produce the same average output value. This range is known as a dead zone.

Consider a first-order SDM with a lossy integrator, such that Eq. (16) is replaced by

$$u(n) = cu(n-1) + x(n) - y(n-1) \quad (39)$$

where  $c < 1$ . For  $x \ll 1$ ,  $y(0) = +1$ , this yields,

$$\begin{aligned} u(1) &= cu(0) + x - y(0) = x - 1 < 0 \\ u(2) &= cu(1) + x - y(1) = (1+c)x + (1-c) > 0 \\ u(3) &= cu(2) + x - y(2) = (1+c+c^2)x - (1-c-c^2) < 0 \end{aligned} \quad (40)$$

which gives the output bitstream  $y(n) = +1, -1, +1, -1, \dots$ . The general formula for the input to the quantizer becomes,

$$u(k) = \sum_{i=0}^{k-1} c^i x + (-1)^k (-c)^i \quad (41)$$

When  $x$  is equal to 0, and  $c < 1$ , then this produces the limit cycle  $+1, -1$ . In order to break out of this limit cycle for nonzero  $x$ , at some point we must have, for odd  $k$ ,

$$u(k) > 0 \rightarrow \sum_{i=0}^{k-1} c^i x > \sum_{i=0}^{k-1} (-c)^i \quad (42)$$

or for even  $k$ ,

$$u(k) < 0 \rightarrow \sum_{i=0}^{k-1} c^i x < -\sum_{i=0}^{k-1} (-c)^i \quad (43)$$

In the limit of large  $k$ , these formulas become

$$\frac{x}{1-c} > \frac{1}{1+c} \text{ and } \frac{x}{1-c} < \frac{-1}{1+c} \quad (44)$$

That is, all input in the range

$$\frac{c-1}{1+c} < x < \frac{1-c}{1+c} \quad (45)$$

will not break out of a limit cycle, and thus will have no effect on the output. The region of input defined by Eq. (45) is known as a dead zone, and the phenomenon is sometimes referred to as a threshold effect. It is strongly

related to limit cycles in that the output is an endlessly repeating bitstream.

A formal definition would be that a dead zone is a continuous range of SDM input, such that, for given initial conditions, the same output bitstream would be produced.

If one considers a nonzero initial condition, then Eq. (41) becomes

$$u(k) = c^k u(0) + \sum_{i=0}^{k-1} c^i x + (-1)^k (-c)^i \quad (46)$$

which in the limit of large  $k$  still reduces to Eq. (41). Thus, this dead zone is independent of initial conditions.

It should be mentioned that in a first-order SDM, dead zones occur for every limit cycle. Since the limit cycles exist with any rational input, this can be rephrased as stating that dead zones exist in the neighborhood of every rational input. Similar phenomena exist in second-order SDMs. Fig. 17 depicts the average output of a sigma-delta modulator as a function of DC input. It can be seen that both first- and second-order SDMs may exhibit dead zones.

Dead zones are familiar to the SDM community and are mentioned in many design textbooks [31]. There was some extensive analysis of dead zones in first- and second-order SDMs in the work of Feely [32-36]. However, she did not refer to them as such, and instead discussed the staircase structure of the SDM output as a function of input, which characterizes the dead zones.

To date, no one who has characterized the dead zones that can exist in high-order SDMs nor fully characterized the possible relationships between dead zones, initial conditions, and input. However, though this seems tractable, there is little evidence that dead zones are a serious issue in high-order SDM designs.

### Stability

In our earlier introduction to the issues in SDM, we stated that the primary reason that ideal SNRs are not achieved with high-order SDMs is that many designs are highly unstable. There has been much research into stability issues in SDMs, but many essential questions remain unsolved. At its core, one would like to derive

values of constant input such that, for certain initial conditions, the magnitude of the quantizer input will diverge toward infinity. A similar question is, given initial conditions and constant input, determine if this leads to stable behavior.

For the first-order SDM, it is easy to show that it is stable for all input  $-1 < x < 1$  and to find the related bitstream behavior. Returning to the time-domain expression given by Eq. (16), assume  $x$  is constant and  $-1 < x < 1$ . The following 2 relationships show that a negative  $u$  will increase until it is positive, and a positive  $u$  will decrease until it is negative.

$$\begin{aligned} u(n) < 0 \Rightarrow u(n+1) &= u(n) + x + 1 > u(n) \\ u(n) \geq 0 \Rightarrow u(n+1) &= u(n) + x - 1 < u(n) \end{aligned} \quad (47)$$

Thus it is oscillating between positive and negative values. Now assume that at least one bit flip has occurred (i.e., the transient behavior has passed and we are not starting from arbitrary initial conditions). From Eq. (47), the maximum value of  $u$  occurs when the previous value is just below zero and the minimum value occurs when the previous value is equal to zero

$$\begin{aligned} u(n) \xrightarrow{<} 0 \Rightarrow u(n+1) &= x + 1 \\ u(n) = 0 \Rightarrow u(n+1) &= x - 1 \end{aligned} \quad (48)$$

Thus  $u$  is limited to the range  $[-1+x; 1+x]$ .

The first-order SDM can be iterated to give, when the output bits all have the same sign,

$$u(n+m) = u(n) + m(x - y) \quad (49)$$

Assume that there are exactly  $n^+$  positive output bits in a row. Then we have

$$u(1) \geq 0$$

...

$$u(n^+) = u(1) + [n^+ - 1](x - 1) \geq 0 \quad (50)$$

Since the maximum value of  $u$  is  $x+1$ , we have that the maximum number of output bits occurs when,

$$x + 1 + [n^+ - 1](x - 1) \geq 0 \quad (51)$$

so the maximum number of positive output bits is given by the largest  $n^+$  such that

$$n^+ \leq \frac{2}{1-x} \quad (52)$$

similarly, the maximum number of negative output bits is given by the

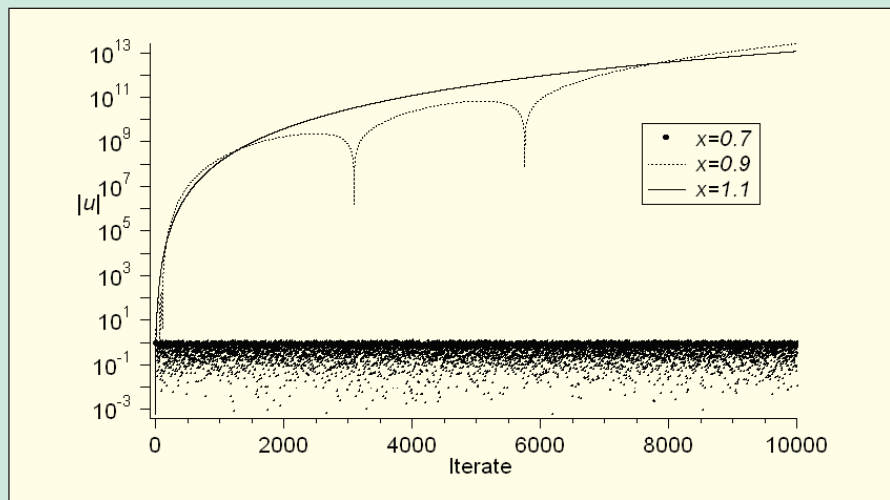


Fig. 18. The absolute magnitude of the quantizer input in a fifth-order SDM as a function of iterate for various constant input magnitudes. At  $x=0.7$ , the quantizer input is stable, at  $x=0.9$  the quantizer input is unstable and oscillating with exponentially increasing period and amplitude, and at  $x=1.1$  the quantizer input is unstable but nonoscillating.

largest  $n^-$  such that

$$n^- \leq \frac{2}{1+x} \quad (53)$$

The standard second-order SDM has similar stability properties in that stability is independent of initial conditions, but proof of boundedness is not trivial. A linear programming approach is used by Farrell and Feely [37]. They assume that there have been some number  $n^-$  iterations with negative output. From this, they identify the maximum values of the state-space variables for the first positive output bit. This value is used to identify the maximum number of positive output bits, which results in  $n^+$ . They then find the maximum number of negative output bits that result from the  $n^+$  positive bits. This new value of  $n^-$  is strictly less than  $n^+$  and hence the oscillations are bounded. This successfully finds the bounds on the second-order SDM and may be extended to second-order SDMs with leaky or chaotic integrators, and their results bear strong agreement with simulation.

To the best of our knowledge, there is no successful analytical approach to stability in high-order SDMs (order greater than 2). There are several alternative approaches to stability in second-order SDMs, some preliminary work on third-order designs, and only sketched approaches to stability in higher-order SDMs. Thus the question becomes, "Can any existing approaches be extended to higher-order SDMs?" Of course, there is the related question of whether existing approaches are correct.

Risbo [38] discussed stability of SDMs in detail, primarily from a nonlinear dynamics perspective. But, with the exception of first-order SDMs, he did not attempt a method for its determination. A computational approach to finding the invariant sets, which consist of initial conditions giving rise to stable behavior, is derived by Schreier [39–41]. Although neither analytical nor rigorous, it is significant because source code is available and because results are provided that may be confirmed or denied by other methods. Hein and Zakhor's approach [42] is to use the limit cycles as a measure of stability. Their method is not rigorous, in that it postulates that the limit cycles have a convergent bound on the state-space variables, and that this is also the bound for nonlimit cycle behavior. Wang [43] converted a third-order modulator to a continuous-time system by looking at the vector field equations. By considering only boundary points, he is able to convert the 3-dimensional flow into a 2-dimensional return map. Fixed points of this map then yield insight into stability of the SDM. Zhang [44, 45] used a model of the quantizer to estimate the stability of a third-order SDM. The linearization implies that important phenomena have been

omitted. Furthermore, there is little comparison of the results with simulation. Another work by Zhang [46] bears a strong resemblance to the linear programming approach of Feely.

Steiner and Yang [47, 48] use a transformation that decouples the state-space variables, except through their interaction in the quantization function. They suggest how this may be used to tackle stability but there is little analysis. This approach has been expanded by Wong [49] to deal with practical high-order SDMs. Wong provides simulated results for many high-order SDMs, but his analysis does not confirm simulation. Mladenov et al. [50] also use a related transformation and have shown promising results on simple but high-order SDMs. The author and collaborators are currently investigating the potential of this technique.

Now we will show that the state-space variables are always unbounded for  $|u|>1$ , and that the state-space variables oscillate between positive and negative values for  $|u|<1$ . Note that this oscillation does not guarantee stable behavior, but an understanding of the oscillations may lead to an understanding of stability.

Returning to the arbitrary SDM given by Eq. (28), it is easy to see that

$$\begin{aligned}s_i(n) > 0 \Rightarrow s_{i+1}(n+1) &> s_{i+1}(n) \\ s_i(n) < 0 \Rightarrow s_{i+1}(n+1) &< s_{i+1}(n)\end{aligned}\quad (54)$$

If  $x>1$ ,  $x-y(n)>0$ , regardless of  $c$ . Therefore,  $s_1(n+1)>s_1(n)$ , e.g.,  $s_1$  always increases. Hence, for some  $k$ ,  $s_1(k)>0$ . At which point  $s_2$  will increase, and at some point it will become positive, and so on. This implies that, at some point all state-space variables will increase. Similarly, if  $x<-1$ , at some point, all state-space variables will decrease. Thus, for any feedforward SDM in this form, the bounds are always  $<-1$ .

Assume  $0<x<1$ , Assume  $y(n)>0$ . So

$$s_1^{(n+1)} = s_1^{(n)} + x - 1 < s_1^{(n)} \quad (55)$$

So  $s_1$  decreases.  $s_2$  may still increase, but eventually  $s_1$  becomes less than 0. Then  $s_2$  starts to decrease, and so on. Eventually  $s_N^{(n)}<0$ , and  $y(n)$  flips to -1. Now, the same procedure happens again, but with each variable increasing. This gives oscillation. The prob-

lem comes when each oscillation takes longer than the previous one. An example of this oscillation is depicted in Fig. 18. For  $x=0.9$ , the system is unstable but still oscillating between -1 and +1 output, though the oscillations are exponentially increasing in both amplitude and period.

## CONCLUSION

In this tutorial we have discussed methods of operation, design, and use of sigma-delta modulators. Although we considered the design of a sigma-delta modulator as used for analog-to-digital conversion, the results derived here could easily be generalized. The descriptions apply equally for SDMs used in other applications, such as D/A converters or Class D amplifiers. The SNR formulas in the linear model and pulse-code modulation section and the section on noise shaping and oversampling can also be modified for different input signals or filter designs. The examples in the section on SDM issues could apply to multibit SDMs as well.

We've identified several key issues in sigma-delta modulation: limit cycles, idle tones, dead zones, harmonic distortion, noise modulation, and stability. To some extent limit cycles may be considered a mostly solved problem, whereas for each of the other problems the issues are understood for low-order design but the theory is not yet established for the high-order designs. Dead zones have been effectively characterized for low-order designs, but they have not been reported to be problematic in high-order or commercial designs. Noise modulation is well understood for PCM, yet there is no well established theory for even low-order sigma-delta modulators. Idle tones and harmonic distortion, though not well understood, are clearly related phenomena. With idle tones in particular, well-defined and simple relationships between the input signal and the frequencies of the tones have been observed that do not yet have a theoretical basis.

Noise modulation, idle tones, harmonic distortion, and limit cycles may be dealt with, at least in part, through the application of dither. However, dither is less effective when

used with a low bit quantizer, which is also when these issues are most serious. Furthermore, dither is not helpful in dealing with stability issues, and will actually decrease the stable range of a sigma-delta modulator. A better understanding of stability (and of other issues) is needed so that robust, high-performance implementations may be developed. There have been many promising recent results that may lead toward a theory of stability in sigma-delta modulators; this remains an active area of investigation for the author.

## REFERENCES

- [1] S. P. Lipshitz, R. A. Wannamaker, and J. Vanderkooy, "Quantization and Dither: A Theoretical Survey," *J. Audio Eng. Soc.*, vol. 40, pp. 355–375 (1992 May).
- [2] S. H. Ardalan and J. J. Paulos, "An Analysis of Nonlinear Behavior in Delta-Sigma Modulators," *IEEE Trans. on Circuits and Systems I: Fundamental Theory and Applications*, vol. 34, pp. 593–603 (1987).
- [3] D. Reefman and E. Janssen, "Signal Processing for Direct Stream Digital: A Tutorial for Digital Sigma-Delta Modulation and 1-Bit Digital Audio Processing," Philips Research, Eindhoven, White Paper 18 (2002 Dec.).
- [4] D. Reefman and P. Nijtjen, "Why Direct Stream Digital (DSD) Is the Best Choice as a Digital Audio Format," presented at the 110th Convention of the Audio Engineering Society, *J. Audio Eng. Soc. (Abstracts)*, vol. 49, p. 545 (2001 Jun.), convention paper 5396.
- [5] D. Reefman, J. Reiss, E. Janssen, and M. Sandler, "Description of Limit Cycles in Sigma-Delta Modulators," *IEEE Trans. on Circuits and Systems I: Regular Papers*, vol. 52, pp. 1211–1223 (2005).
- [6] J. D. Reiss and M. B. Sandler, "They Exist: Limit Cycles in High Order Sigma-Delta Modulators," presented at the 114th Convention of the Audio Engineering Society, *J. Audio Eng. Soc. (Abstracts)*, vol. 51, p. 436 (2003 May), convention paper 5832.
- [7] D. Reefman, J. D. Reiss, E. Janssen, and M. B. Sandler, "Stability Analysis of Limit Cycles in High Order Sigma-Delta Modulators," presented at

the Audio Engineering Society 115th Convention, *J. Audio Eng. Soc. (Abstracts)*, vol. 51, p. 1240 (2003 Dec.), convention paper 5936.

[8] J. D. Reiss and M. B. Sandler, "A Mechanism for the Detection and Removal of Limit Cycles in the Operation of Sigma-Delta Modulators," British Patent Application No. 0514677.4, UK patent filed July 18th 2005.

[9] J. D. Reiss and M. Sandler, "The Harmonic Content of a Limit Cycle in a DSD Bitstream," presented at the Audio Engineering Society 116th Convention, *J. Audio Eng. Soc. (Abstracts)*, vol. 52, p. 806 (2004 Jul./Aug.), convention paper 6092.

[10] D. Reefman, J. D. Reiss, E. Janssen, and M. Sandler, "Description of Limit Cycles in Feedback Sigma-Delta Modulators," presented at the Audio Engineering Society 117th Convention, *J. Audio Eng. Soc. (Abstracts)*, vol. 53, p. 110 (2005 Jan./Feb.), convention paper 6280.

[11] A. Gothenberg and H. Tenhunen, "Improved Cascaded Sigma-Delta Noise Shaper Architecture with Reduced Sensitivity to Circuit Nonlinearities," *Electronics Letters*, vol. 38, pp. 683–685 (2002).

[12] C. Y.-F. Ho, B. W.-K. Ling, and J. D. Reiss, "Fuzzy Impulsive Control of High Order Interpolative Lowpass Sigma-Delta Modulators," to appear in *IEEE Trans. on Circuits and Systems-I: Regular Papers* (2005).

[13] J. C. Candy and O. J. Benjamin, "The Structure of Quantization Noise from Sigma-Delta Modulation," *IEEE Trans. Commun.*, vol. COM-29, pp. 1316–1323 (1981).

[14] A. J. Magrath and M. B. Sandler, "Efficient Dithering of Sigma-Delta Modulators with Adaptive Bit Flipping," *Electronics Letters*, vol. 31 (1995).

[15] R. Schreier, "On the Use of Chaos to Reduce Idle-Channel Tones in Delta-Sigma Modulators," *IEEE Trans. on Circuits and Systems I*, vol. 147, pp. 539–547 (1994).

[16] J. M. de la Rosa, B. Perez-Verdu, F. Medeiro, R. del Rio, and A. Rodriguez-Vazquez, "Analysis and Experimental Characterization of Idle Tones in 2nd-Order Bandpass Sigma-Delta Modulators—A 0.8  $\mu$ m CMOS Switched-Current Case

Study," *Proc. IEEE Int. Sym. on Circuits and Systems*, ISCAS 2001, pp. 774–777 (2001).

[17] M. Kozak and I. Kale, *Oversampled Delta-Sigma Modulators: Analysis, Applications and Novel Topologies* (Kluwer Academic Publishers, Dordrecht, The Netherlands, 2003).

[18] G. I. Bourdopoulos, A. Pnevmatikakis, V. Anastassopoulos, and T. L. Deliyannis, *Delta-Sigma Modulators: Modeling, Design and Applications* (Imperial College Press, London, UK, 2003).

[19] R. C. Ledzius and J. Irwin, "The Basis and Architecture for the Reduction of Tones in a Sigma-Delta DAC," *IEEE Trans. on Circuits and Systems - II, Analog and Digital Signal Processing*, vol. 40 (1993).

[20] J. A. S. Angus, "The Effect of Noise Transfer Function Shape on Idle Tones in Sigma-Delta Modulators," presented at the 118th Convention of the Audio Engineering Society, *J. Audio Eng. Soc. (Abstracts)*, vol. 53, p. 694 (2005 Jul./Aug.), convention paper 6450.

[21] P. A. G. Jespers, *Integrated Converters: D to A and A to D Architectures, Analysis and Simulation* (Oxford University Press, Oxford, UK, 2001).

[22] E. Perez Gonzalez and J. D. Reiss, "Idle Tone Behavior in Sigma-Delta Modulation," Audio Engineering Society 122nd Convention Papers CD-ROM (2007 May), convention paper 7108 in AES E-Library <[www.aes.org/e-lib](http://www.aes.org/e-lib)>.

[23] C. Dunn and M. Sandler, "A Comparison of Dithered and Chaotic Sigma-Delta Modulators," *J. Audio Eng. Soc.*, vol. 44, pp. 227–244 (1996).

[24] J. M. de la Rosa, B. Perez-Verdu, F. Medeiro, R. del Rio, and A. Rodriguez-Vazquez, "Effect of Non-linear Settling Error on the Harmonic Distortion of Fully-Differential Switched-Current Bandpass Sigma-Delta Modulators," *Proc. IEEE International Symposium on Circuits and Systems*, ISCAS 2001, pp. 340–343 (2001).

[25] S. R. Norsworthy, I. G. Post, and H. S. Fetterman, "A 14-Bit 80-kHz Sigma-Delta A/D Converter: Modeling, Design and Performance

Evaluation," *IEEE J. Solid-State Circuits*, vol. 24, pp. 256–266 (1989).

[26] F. Op't Eynde, P. Meulemans, F. Heyrman, B. Maes, and W. Sansen, "A Calculation Method to Predict In-Band Harmonic Distortion of Sigma-Delta D/A Converters," *Proc. IEEE Int. Sym. on Circuits and Systems*, pp. 671–674 (1989).

[27] V. F. Dias, G. Palmisano, and F. Maloberti, "Harmonic Distortion in SC Sigma-Delta Modulators," *IEEE Trans. on Circuits and Systems I: Fundamental Theory and Applications*, vol. 41, pp. 326–329 (1994).

[28] R. T. Baird and T. S. Fiez, "Linearity Enhancement of Multibit Sigma-Delta A/D and D/A Converters Using Data Weighted Averaging," *IEEE Trans. on Circuits and Systems II: Analog and Digital Signal Processing*, vol. 42, pp. 753–762 (1995).

[29] S. P. Lipshitz and J. Vanderkooy, "Why Professional 1-Bit Sigma-Delta Conversion Is a Bad Idea," presented at the Audio Engineering Society 109th Convention, *J. Audio Eng. Soc. (Abstracts)*, vol. 48, p. 1099 (2000 Nov.), convention paper 5188.

[30] J. D. Reiss and M. Sandler, "Dither and Noise Modulation in Sigma-Delta Modulators," presented at the Audio Engineering Society 115th Convention, *J. Audio Eng. Soc. (Abstracts)*, vol. 51, p. 1239 (2003 Dec.), convention paper 5935.

[31] R. Schreier and G. C. Temes, *Understanding Delta-Sigma Data Converters* (John Wiley and Sons, Hoboken, NJ, USA, 2005).

[32] O. Feely and L. O. Chua, "The Effect of Integrator Leak in S-D Modulation," *IEEE Trans. on Circuits and Systems*, vol. CAS-38, pp. 1293–1305 (1991).

[33] O. Feely and L. O. Chua, "Nonlinear Dynamics of a Class of Analog-to-Digital Converters," *Int. J. Bifurcation and Chaos*, vol. 2, pp. 325–340 (1992).

[34] O. Feely and L. O. Chua, "Multilevel and Non-Ideal Quantization in Sigma-Delta Modulation," *Int. J. of Circ. Theory and Appl.*, vol. 21, pp. 61–83 (1993).

[35] O. Feely, "A Tutorial Introduction to Non-Linear Dynamics and Chaos and their Application to

Sigma-Delta Modulators," *Int. J. Circ. Theory and Appl.*, vol. 25, pp. 347–367 (1997).

[36] O. Feely, "Nonlinear Dynamics of Sigma-Delta Modulators and Phase-Locked Loops," Queen Mary University of London, London, UK, invited talk (2002 Jan.).

[37] R. Farrell and O. Feely, "Bounding the Integrator Outputs of Second Order Sigma-Delta Modulators," *IEEE Trans. on Circuits and Systems, Part II: Analog and Digital Signal Processing*, vol. 45, pp. 691–702 (1998).

[38] L. Risbo, "Sigma-Delta Modulators—Stability Analysis and Optimization," PhD Thesis, Electronics Institute, Technical University of Denmark, 1994, pp. 179, (1994) <<http://eivind.imm.dtu.dk/publications/phdthesis.html>>.

[39] R. Schreier, M. Goodson, and B. Zhang, "An Algorithm for Computing Convex Positively Invariant Sets for Delta-Sigma Modulators," *IEEE Trans. on Circuits and Systems I: Fundamental Theory and Applications*, vol. 44, pp. 38–44 (1997).

[40] B. Zhang, M. Goodson, and R. Schreier, "Invariant Sets for General Second-Order Lowpass Delta-Sigma Modulators with DC Inputs," *Proc. ISCAS*, pp. 1–4 (1994).

[41] M. Goodson, B. Zhang, and R. Schreier, "Proving Stability of Delta-Sigma Modulator Using Invariant Sets," *Proc. ISCAS*, pp. 633–636 (1995).

[42] S. Hein and A. Zakhor, "On the Stability of Sigma-Delta Modulators," *IEEE Trans. Signal Processing*, vol. 41, pp. 2322–2348 (1993).

[43] H. Wang, "On the Stability of Third-Order Sigma-Delta Modulation," *Proc. ISCAS*, pp. 1377–1380 (1993).

[44] J. Zhang, P. V. Brennan, D. Jiang, E. Vinogradova, and P. D. Smith, "Stable Boundaries of a Third-Order Sigma-Delta Modulator," *Proc. Southwest Symp. on Mixed-Signal Design*, pp. 259–262 (2003).

[45] J. Zhang, P. V. Brennan, D. Jiang, E. Vinogradova, and P. D. Smith, "Stability Analysis of a Sigma-Delta Modulator," *Proc. Int. Symp. on Circuits and Systems, ISCAS*, pp. I-961–I-964 (2003).

[46] J. Zhang, P. V. Brennan, P. D. Smith, and E. Vinogradova, "Bounding Attraction Areas of a Third-Order Sigma-Delta Modulator," *Proc. Int. Conf. on Communications, Circuits and Systems, ICCCAS*, pp. 1377–1381 (2004).

[47] P. Steiner and W. Yang, "A Framework for Analysis of High-Order Sigma-Delta Modulators," *Circuits and Systems II: Analog and Digital Signal Processing, IEEE Trans.*, pp. 1–10 (1997).

[48] P. Steiner and W. Yang, "Stability of High Order Sigma-

Delta Modulators," *Proc. IEEE Int. Symp. on Circuits and Systems, ISCAS'96*, pp. 52–55 (1996).

[49] N. Wong and T.-S. Tung-Sang Ng, "DC Stability Analysis of High-Order, Lowpass Sigma-Delta Modulators With Distinct Unit Circle NTF Zeros," *IEEE Trans. On Circuits And Systems-II: Analog And Digital Signal Processing*, vol. 50 (2003).

[50] V. Mladenov, H. Hegt, and A. V. Roermund, "On the Stability Analysis of High Order Sigma-Delta Modulators," *Analog Integrated Circuits and Signal Processing*, vol. 36 (2003).

## THE AUTHOR



**Joshua D. Reiss** was born in 1971, and is a Lecturer with the Centre for Digital Music and the Digital Signal Processing group in the Electronic Engineering department at Queen Mary, University of London. He has bachelor's degrees in both physics and mathematics, and received his Ph.D. in physics from the Georgia Institute of Technology, specializing in the analysis of chaotic time series.

In June of 2000, he accepted a research position in the Audio Signal Processing research lab at King's College, London, and moved to Queen Mary in 2001. He made the transition from chaos theory to audio processing through his work on sigma-delta modulators, which has lead to a nomination for a best paper award from the IEEE, as well as a UK patent. His work also includes significant contributions to the fields of

music retrieval and processing, audio effects, satellite navigation, and nonlinear dynamics.

Reiss is very active in the Audio Engineering Society, including being a member of the Review Board for the *Journal* and vice chair of the Technical Committee on High-Resolution Audio. He was on the Organizing Committee of DAFX2003 and MIREX2005 and was recently program chair for the 2005 International Conference on Music Information Retrieval and general chair of the 2007 AES International Conference on High Resolution Audio. As coordinator of the EASAER project, he leads an international consortium of seven partners working to improve access to sound archives in museums, libraries, and cultural heritage institutions.